Elevated levels of the small GTPase Cdc42 induces senescence in male rat mesenchymal stem cells

Bauyrzhan Umbayev[1] • Abdul-Razak Masoud [1] • Andrey Tsoy[1] • Dauren Alimbetov[1] • Farkhad Olzhayev[1] •Alla Shramko • Aiym Kaiyrlykyzy[1] •, Yulia Safarova[1] • Terence Davis[2] • Sholpan Askarova[1] (✉)

[1]*Laboratory of bioengineering and regenerative medicine, Center for Life Sciences, National Laboratory Astana, Nazarbayev University, 53 Kabanbay Batyr Ave, Z05H0P9 Astana, Kazakhstan.*
[2]*Division of Cancer and Genetics, Cardiff University School of Medicine, Heath Park, Cardiff CF14 4XN, UK.*

(✉) Correspondence: Ph. +77172706514, Email: shaskarova@nu.edu.kz

Abstract

Mesenchymal stem cells (MSCs) represent a promising cell source for cellular therapy and tissue engineering and are currently being tested in a number of clinical trials for various diseases. However, like other somatic cells, MSCs age, and this senescence is accompanied by a progressive decline in stem cell function. Several lines of evidence suggest a role for the Rho family GTPase Cdc42 activity in cellular senescence processes. In the present study, we have examined aging-associated Cdc42 activity in rat adipose-derived mesenchymal stem cells (ADMSCs) and the consequences of pharmacological inhibition of Cdc42 in ADMSCs from aged rats. We demonstrate that ADMSCs show a decreased rate of cell growth and a decreased ability to differentiate into chrodrogenic, osteogenic and adipogenic cell lineages as a function of rat age. This is accompanied with an increased staining for SA-β-Gal activity and increased levels of Cdc42 bound to GTP. Treatment of ADMSCs from 24-month old rats with three Cdc42 inhibitors significantly increased proliferation rates, decreased SA-β-Gal staining, and reduced Cdc42-GTP. The Cdc42 inhibitor CASIN increased adipogenic and osteogenic differentiation potential in ADMSCs from 24-month old rats, and decreased the levels of radical oxygen species (ROS), $p16^{INK4a}$ levels, F-actin, and the activity of the ERK1/2 and JNK signaling pathways that were all elevated in these cells. These data suggest that ADMSCs show increased rates of senescence as rats age that appear to be due to elevated Cdc42 activity. Thus, Cdc42 plays important roles in MSC senescence and differentiation potential, and pharmacological reduction of Cdc42 activity can, at least partially, rejuvenate aged MSCs.

Keywords

CASIN • Cdc42 • c-Jun N-terminal kinase • cell proliferation • differentiation • ERK1/2 • ML141 •MSC • SA-β-Galactosidase • senescence • ZCL278

Introduction

Mesenchymal stem cells (MSCs) represent a promising cell source for cellular therapy and tissue engineering due to their ability to proliferate and differentiate into various cell types, including those that make up tissues such as bone, ligament, tendon, cartilage and adipose (Cheng et al. 2013; Fernandez Vallone et al. 2013). MSCs are currently being tested in a number of clinical trials for various diseases that include myocardial infarction, stroke, diabetes and cartilage

defects (Kramer et al. 2012; Wang et al. 2012a). However, there are some limitations for therapeutic use of MSCs. In the case of allogeneic transplantation of MSCs from healthy young donors, the production of the desired quantity and quality of MSCs needed for clinical application mostly depends upon culture conditions (Chen et al. 2009; Sotiropoulou et al. 2006), while autologous therapy is also limited by the patient's age (Dai et al. 2009; Mareschi et al. 2006). Like other somatic cells, MSCs age, and this senescence is accompanied by a progressive decline in stem cell function. In addition, the ability of human MSCs to divide reduces with age of the individual (Mareschi et al. 2006). Aged MSCs can share many characteristics of aged somatic cells, including reduced replicative potential, reduced telomere length, enlarged cell morphology with stress fibres, and the production of inflammatory markers (Sethe et al. 2006). These aged cells also have a reduced ability to differentiate into various tissue types (Sethe et al. 2006). However, although understanding the basic molecular mechanisms of stem cell aging has significant implications for regenerative medicine and stem cell therapy, the mechanisms of MSC aging remain obscure (Lee et al. 2006; Mareschi et al. 2006; Sethe et al. 2006; Yue et al. 2005).

There is evidence suggesting the involvement of a small Rho family GTPase, Cdc42, also known as cell division control protein 42 homolog, in cell aging and senescence-associated inflammation (Ito et al. 2014; Kerber et al. 2009; Wang et al. 2007). Elevated levels of activated Cdc42 (Cdc42 bound to GTP) are associated with various age-related pathologies, including reduced lifespan, reduced wound healing, muscle wasting, atherosclerosis and osteoporosis (Ito et al. 2014; Wang et al. 2007), and are associated with carcinogenesis, diabetes, cardiovascular and neurodegenerative diseases (Hooff et al. 2010; Lee et al. 2014; Loirand et al. 2013; Raut et al. 2015; Stengel and Zheng 2011). At a cellular level increased Cdc42-GTP results in up-regulation of senescence related proteins such as p53, $p21^{WAF1}$ and $p16^{INK4a}$ in mouse embryonic fibroblasts and human endothelial cells (Ito et al. 2014; Wang et al. 2007) and the activation of stress related MAP kinase pathways such as p38 that can lead to increased inflammatory markers in IMR-90 foetal lung cells (Chretien et al. 2008).

In human adult-derived MSCs Cdc42 plays multiple regulatory roles, including in the processes of osteogenic and adipogenic differentiation (Gao et al. 2011; Jirong Wang 2014; Shin et al. 2014), and elevated Cdc42-GTP levels lead to MSC morphology changes and elevated F-actin stress fibres that are features associated with cellular senescence (Xu et al. 2017). In addition, an altered microenvironment causes an increased expression of Cdc42 in mouse MSCs that may lead to senescent-like changes (McGrail et al. 2012), and with advancing adult age there is an increasing deficit of cellular proliferation and signal transduction control in MSCs that leads to adipogenic differentiation (Raggi and Berardi 2012).

The above data, taken together with the observation that elevated Cdc42 activity in aged mouse hematopoietic stem cells (HSCs) is causally linked to HSC aging, and correlates with a loss of polarity in aged HSCs (Florian et al. 2012), suggest that Cdc42-GTP activity may be involved in MSC senescence and differentiation potential. Any up-regulation of Cdc42-GTP activity may, in turn, be associated with difficulties obtaining MSCs for therapeutic use (Dai et al. 2009; Mareschi et al. 2006). Thus, in the present study, we have examined aging-associated Cdc42 activity in adipose-derived MSCs isolated from rats of different ages and tested the effects of pharmacological inhibition of Cdc42 in MSCs isolated from aged animals.

Materials and Methods

Animals

1, 3, 6, 12 and 24 months old male Wistar rats were used in this study. The rats were housed in cages with controlled temperature (22 ± 2°C), relative humidity (55 ± 10%) and a 12-hour light/dark cycle (07:00 to 19:00 light) with free access to water and a standard rat diet. All the experiments were performed in accordance with the ethical guidelines of the U.S. Department of Health and Human Services (HHS), Registration of an Institutional Review Board (IRB) and approved by the Ethics Committee of the Center for Life Sciences of Nazarbayev University (Registration number IORG 0006963).

Adipose-derived mesenchymal stem cell isolation and characterization

Isolation and characterization of adipose-derived MSCs (ADMSCs) was performed according to previously described protocol (Arana et al. 2013) with minor modifications. The procedure used here is fully described in the Supplementary Methods. ADMSCs are herein defined as CD105-sorted cells that have been subsequently cultured for 4-5 passages and are $CD31^-$, $CD34^-$, $CD45^-$, $CD90^+$ and $CD105^+$ (see Supplementary Methods and Figures).

Culture medium

ADMSCs were routinely cultured in Dulbecco's Modified Eagle Medium (DMEM) containing 15% FBS and 1% Penicillin/streptomycin (herein called Complete Medium), unless otherwise stated.

Multipotent Differentiation of ADMSCs

CD105 sorted ADMSCs (passage 4) were plated in 6-well plates at a density of 20,000 cells/cm^2 for adipogenesis, 10,000 cells/cm^2 for osteogenesis and chondrogenesis and grown until 80% confluence prior to starting differentiation. Osteogenic differentiation of MSCs was induced under the influence of 10 nM β-glycerol phosphate, 0.1 μM dexamethasone, and 100 μM L-ascorbic acid 2 phosphate. Chondrogenic medium consisted of 10 ng/mL TGFβ1, 0.1 μM dexamethasone, 50 g/mL ascorbate-2-phosphate, 40 mg/mL proline, and 50 mg/mL Insulin-Transferrin-sodium selenite. Adipogenic medium contained 1 μM dexamethasone, 5 ng/ml insulin, and 0.5 μM 3-isobutyl-1-methylxanthine. Differentiation media was replaced every 3 days for a total of 21 days. Cells incubated in osteogenic, chondrogenic and adipogenic media were fixed in 4% formaldehyde and stained with 40 mM Alizarin Red S, 1% alcian blue and Oil Red O, respectively.

Quantification of adipocyte differentiation

ADMSCs that had undergone adipogenic differentiation were fixed in 4% formaldehyde for 1 hr, washed with 60% isopropanol and stained with Oil Red O solution (in 60% isopropanol) for 5 mins followed by repeated washing with PBS. After microscopic observation, Oil Red O was destained by 100% isopropanol for 15 mins and aspirates were collected for further analysis (Bony et al. 2015). The optical density (O.D.) of the isopropanol containing Oil Red O was measured at 540 nm with Synergy Hybrid H1 Microplate Reader (Biotek, USA).

Quantification of osteogenic differentiation

Osteogenic differentiation was evaluated with Alizarin red staining for calcium deposition. Briefly, ADMSCs were fixed in 4% formaldehyde for 15 minutes, stained with 40 mM of Alizarin Red S for 30 mins, incubated in 10% acetic acid and collected using a cell scraper into the micro centrifuge tubes. After centrifugation supernatants were transferred to new tubes and 10% ammonium hydroxide was added to neutralize the acid while ensuring the pH ranged between 4.1 and 4.5. O.D of the Alizarin red was measured at 405 nm with Synergy Hybrid H1 Microplate Reader. The Alizarin red concentrations were calculated based on the standard curve.

Cell proliferation

ADMSC suspensions were seeded at 5000 cells/well in a 48-well plate in Complete Medium and continuously incubated for 24 - 120 hrs in a humid incubator at 37^0C, 5% CO_2. ADMSC proliferation rates were analyzed using a cell counting kit-8 (CCK-8, Sigma-Aldrich) according to the assay protocol. The volume of cell counting kit solution added to each well amounted to 10% of the total volume of solution in the well. The plate was incubated for 2 hrs in an incubator at 37^oC with 5% CO_2. 100 µl of suspension was collected from each well, pipetted into a 96-well plate and the absorbance measured at 450 nm using a Synergy Hybrid H1 Microplate Reader (Biotek, USA) at 24 hrs intervals.

Experiments with Cdc42 inhibitors

ADMSCs were cultured for 16 hrs in complete culture medium containing one of the following Cdc42 inhibitors: CASIN (5µM, Sigma Aldrich), ML141 (10µM, Sigma Aldrich), ZCL278 (25µM , Sigma Aldrich). The cells were washed in PBS and subjected for further measurements (Western blot, SA-β-Gal assay, ROS generation analysis, Actin-green and Oil red O and Alizarin Red staining and MAPK assays). For the cell proliferation assay, ADMSC suspensions were seeded at 5000 cells/well in a 48-well plate and cultured for 16 hrs in complete culture medium containing one of the Cdc42 inhibitors, after which the culture medium was replaced with complete medium without inhibitors and the cells incubated for up to 120 hrs.

SA-β-Gal staining

To assess the expression of senescence associated β-galactosidase (SA-β-Gal) in cells a Senescence Cells Histochemical Staining Kit (Sigma Aldrich) was used according to the manufacturer's protocol. Briefly, passage 5 ADMSCs were fixed in Fixation Buffer for 6-7 mins, stained with Staining Mixture and incubated at 37°C without CO_2 overnight. The percentage of cells expressing β-galactosidase was calculated as the ratio of blue-stained cells: total cells × 100 with at least 500 cells counted.

Western blot analysis

Cdc42 levels were measured using a Cdc42 detection kit (Cell Signaling) according to the manufacturer’s protocol. Briefly, ADMSCs were harvested in 0.5 ml lysis buffer containing 1 mM of PMSF. Lysates were collected and the active form of the protein (Cdc42-GTP) was immunoprecipitated using glutathione resin. Extracts containing Cdc42-GTP were sonicated and

resolved by SDS-PAGE gel electrophoresis. After electrophoresis, proteins were transferred to nitrocellulose membranes. The blots were incubated with blocking solution (Tris-buffered saline, pH 7.4, 5% BSA, 0.5% Tween 20 [TBS-T]) for 1 hr at room temperature. Membranes were washed and incubated with mouse anti-Cdc42 antibody (Cell Signaling, 1:200 dilution) overnight at 4ºC. After washing with TBS-T, membranes were incubated with anti-mouse IgG, HRP-linked Antibody (Cell Signaling, 1:2000) and anti-biotin HRP-linked Antibody (cell signaling, 1:1000) for 1 hr at room temperature. Blots were washed 3 times with TBS-T and incubated for 1 min in LumiGLO substrate, scanned in a BioRAD ChemiDoc MP imager and processed using ImageLab software (BioRAD). Ratios of Cdc42-GTP to total Cdc42 were calculated for each sample and normalized to the 1 month's control.

$p16^{INK4a}$ protein expression level was detected at 16 kDa. The ADMSCs were harvested in 700 µL lysis buffer (Cell Signaling Technology, USA). The concentration of the protein in the lysate was determined using BCA protein assay according to the manufacturer's protocol (Pierce BCA Protein Assay Kit, ThermoFisher Scientific USA). Briefly, equal amounts of the lysates (25 µL) with total protein concentrations of 1000 µg/ml were collected, sonicated and separated in a precast PAGE gel (Biorad USA). The separated proteins were then transferred onto an Immun-Blot ® PVDF Membrane (Biorad USA). Blocking was done in Tris buffered saline containing 1% tween 20 (TBS-T) and 5% BSA (Sigma, USA) for 1 hr at room temperature. Then membranes were washed 3 times with TBS-T and incubated with primary $p16^{INK4a}$ Monoclonal Antibody (1:1000, ThermoFisher Scientific) overnight at 4 ^{0}C and goat anti-mouse IgG – horseradish peroxidase (1:500, Santa Cruz) for an hour at room temperature. For quantification, blots were scanned in a BioRAD ChemiDoc MP imager and intensity of protein bands was measured as optical density using the ImageLab software (BioRAD) and normalized to the 1 month's control.

Determination of level of reactive oxygen species (ROS)

The 5-(and 6-)chloromethyl-2',7'-dichlorodihydrofluorescein diacetate (CM-H2DCFDA, Life Technologies) was applied to determine ROS production in the cells. The acetate groups of CM-H2DCFDA cleaved by intracellular esterases react with oxygen radicals to produce highly fluorescent adduct that is traped inside the cells causing an increased fluorescent intensity of the cell. For ROS measurements, cells were seeded in 96 well plates, treated with CASIN in phenol-red free DMEM for 16 hrs, and incubated with CM-H2DCFDA (2.5 µM) for 1 hr. Fluorescent intensity of CM-H2DCFDA were measured using microplate reader Synergy H1.

Labeling of F-actin

For assessment of actin polymerization, ADMSCs were grown on cover slips until 50% confluency. Cells were fixed in 3.7% paraformaldehyde solution for 30 minutes and permeabilized using 0.1% Triton X-100 in PBS for 5 min. Cell labeling was done with Actin-green™ 488 ReadyProbes™ reagent according to manufacturer's protocol (Life Technologies, USA) at room temperature for 30 minutes.

Quantitative immunofluorescence microscopy (QIM)

Bright-field illumination and fluorescence microscopy images were obtained on an Olympus IX83 fluorescence microscope coupled with a cooled CCD camera and analyzed on a computer with a CellSens Dimension imaging software. Fluorescent imaging parameters were set as follows: 20X, NA 0.95 objective; exposure time for image acquisition - 400 msec. Background was subtracted for all images prior to analysis. To quantify actin polymerization, the intensity of Actin-green™ 488 ReadyProbes™-labeled F-actin per cell area was calculated and then normalized by the intensity of the labeled F-actin in control cells (1-month old ADMSCs without treatment).

MAP kinase assays

The total concentration and the phospho-kinase/total kinase ratio for the JNK and ERK1/2 kinases were determined in ADMSC whole cell lysates using MSD MAP Kinase Total and Phosphoprotein Assay Kits (Meso Scale Discovery). All procedures were performed according to the manufacturer's protocol. Briefly, whole cell lysates were prepared using the buffer provided with the kit. Cellular debris was cleared from the lysate by centrifugation at 10,000 x g for 10 min. To make the sandwich for electrochemiluminescence immunoassay cell lysates were added to the wells of plates pre-coated with capture antibodies and incubated for 3 hrs. Afterwards the plates were washed 3 times followed by incubation with detection antibody for 1 hr. After a final wash, 150 μL of Read Buffer was added to each well and the plates analyzed on MSD QuickPlex SQ 120. Bicinchoninic Acid Assay was used as loading control.

Statistical analysis

Data are reported as mean ± SD. Proliferative activity of ADMSCs was tested using two-way ANOVA with post-hoc comparison. A one-way ANOVA and regression analysis were conducted to compare the effect of age on SA-β-Gal staining. In all other experiments the unpaired t-test was applied to test mean differences from at least three independent trials. Values were considered significantly different when $P \leq 0.05$. Statistical analyses were performed with Graphpad Prism 7.1 software.

Results

Characterization of the ADMSC phenotype

Freshly isolated cells from adipose tissue were heterogeneously positive for hematopoietic markers CD34 and CD45, endothelial marker CD31, and mesenchymal markers CD105 and CD90 showing a mixed cell population (data not presented). CD105 sorted cells after being cultured for 4-5 passages were more homogeneous: ~90% of the cells from rats of all age groups were positive for specific mesenchymal CD90 and CD105 markers (Lotfy et al. 2014), and negative for CD34, CD45 and CD31 cell surface markers (Supplementary Figs. 1a, 1b). These cells are thus deemed to be MSCs and are the cells referred to as ADMSCs in this paper.

Differentiation capacity of ADMSCs isolated from rats of different ages

To further provide evidence of the mesenchymal nature of these cells their multi-lineage differentiation potential was evaluated. The passage 4-5 CD105-positive cells were able to differentiate towards osteogenic, chondrogenic and adipogenic lineages (Supplementary Fig. 2). However, visual appearance of Alazarin Red S and alcian blue stained cells revealed reduced osteogenic and chondrogenic differentiation capacities of ADMSCs isolated from 12-24-month old animals (Supplementary Fig. 2). Decreased adipogenic differentiation was confirmed by quantification of Oil Red O (Fig. 1a). Our results indicated that ADMSCs from 1-month old donors accumulated more fat droplets in their cytoplasm after incubation in adipogenic medium and staining with Oil Red O compared to ADMSCs from the 12-month old and 24-month old rats ($P<0.05$, unpaired t-test).

Proliferative activity of ADMSCs isolated from rats of different ages

We measured the proliferative activity of ADMSCs isolated from rats of different ages using the CCK-8 assay (Fig. 1b). The proliferative activity of ADMSCs from all age groups peaked on the second day, after which the cells entered a relatively stationary phase. Both the growth rates and proliferation peaks of ADMSCs decreased with increased age of the animals. ADMSCs isolated from 1-month old rats had significantly greater proliferative capacity than ADSMSCs isolated from older animals.

Expression of SA-β-Galactosidase in ADMSCs isolated from rats of different ages

One widely used biomarker of cell senescence is an increased expression of senescence associated β-galactosidase. Phase contrast images of SA-β-Gal-stained ADMSCs and the percentage of SA-β-Gal-positive cells are shown in Supplementary Fig. 3 and Fig. 1c. One way ANOVA tests revealed significant differences between the ADMSCs from different rat age groups ($P \leq 0.001$). Furthermore, regression analysis showed that the percentage of SA-β-Gal-positive ADMSCs gradually increased from approximately 10% in one month old rats to 50% in rats of 24 months of age (P 0.001).

Expression of Cdc42 in ADMSCs from rats of different ages

Significant correlations have been reported between elevated levels of Cdc42 and loss of polarity, functional deficiencies, and impaired self-renewal capability in mouse hematopoietic stem cells (Florian et al. 2012). It has also been demonstrated that Cdc42 levels vary across age groups in mice (Wang et al. 2007). Western blot analysis showed increased Cdc42-GTP levels in ADMSCs isolated from 6-24 months old rats compared to cells isolated from younger animals, with the highest expression of Cdc42 being detected in ADMSCs of 24-month old animals (Fig. 1d, 1e): indeed there is a progressive increase in Cdc42-GTP levels with increasing age.

Effects of the Cdc42 inhibitor CASIN on the growth kinetics and cellular phenotype of ADMSCs from young and aged rats

We tested the consequences of pharmacological inhibition of Cdc42 in ADMSCs isolated from 24-month old rats in comparison with younger animals (1-month old) using CASIN. Assessments by Western blot showed significantly higher levels of Cdc42-GTP in ADMSCs isolated from 24-month old animals compared to 1-month old rats and a significant reduction of the Cdc42-GTP levels in ADMSCs from both aged and young rats by CASIN (Fig. 2a, 2b).

CASIN did not affect the low levels of expression of SA-β-Gal seen in ADMSCs isolated from 1-month old rats, but significantly decreased the percentage of SA-β-Gal-positive cells in ADMSCs isolated from 24-month old rats compared to untreated control ($P \leq 0.001$; unpaired t-test) (Fig. 2d; Supplementary Fig. 4). However, this treatment did not reduce the level of SA-β-Gal-positive cells to that seen in ADMSCs from young rats (Fig. 1d). ADMSCs from older animals had increased levels of the cyclin-dependent kinase inhibitor $p16^{INK4a}$ compared to cells from younger animals (Fig. 2a, 2c), and CASIN treatment decreased this expression to the level seen in the young control ($P \leq 0.05$; unpaired t-test).

Using CCK-8 analysis to assess ADMSC growth kinetics showed that CASIN improved the impaired proliferative activity of ADMSCs from aged rats (Fig. 2e). However, this treatment did not affect growth the rate of cells from 1-month old animals (Fig. 2f) and was not able to increase the proliferation rate of cells from older animals to the levels seen in ADMSCs from young rats (see Fig. 2e, 2f).

The production of high levels of Reactive Oxygen Species (ROS) has been associated with cellular senescence (Chandrasekaran et al. 2017; Colavitti and Finkel 2005; Davalli et al. 2016). In agreement with previous reports, fluorescent analysis showed an ~60% increase of ROS level in ADMSCs from aged rats compared to younger controls ($P \leq 0.001$; unpaired t-test) (Fig. 2g). This increased ROS production in ADMSCs from aged rats was attenuated by CASIN with no significant effects on CM-H2DCFDA intensity in younger cells.

Impaired actin polymerization is another hallmark of cell senescence (Kasper et al. 2009; Li et al. 2017; Xu et al. 2017), and it can be mediated by the upregulation and activation of Cdc42 (Tang and Gunst 2004; Zlotorynski 2015). We employed QIM of F-actin labeled with Actin-green™ 488 ReadyProbes™ cells to quantify actin polymerization in ADMSCs isolated from young and old animals. QIM data showed that aging promoted actin polymerization in ADMSCs ($P \leq 0.001$; unpaired t-test) while treatment with CASIN reduced F-actin intensity in old cells ($P \leq 0.05$; unpaired t-test) (Fig. 2h and Supplementary Fig. 5.), although not to the level seen in ADMSCs from 1-month old rats, and does not cause a reorganization of the cytoskeleton structure in the younger control.

CASIN increases adipogenic and osteogenic differentiation of ADMSCs from aged rats

A decreased differentiation capacity is a hallmark of MSC aging (Maredziak et al. 2016). Quantitative spectrophotometric analysis of Oil Red O confirmed that the amount of dye in the aspirate collected from the cells of 24-month old rats was 1.8-fold lower ($P<0.05$, unpaired t-test) than the amount collected from cells of young rats (Fig. 1a, 3a). Inhibition of Cdc42 by CASIN

significantly improved the adipogenic differentiation of ADMSCs from the aged rats, although this did not reach the levels seen in ADMSCs from the young rats (Fig. 3a).

Similarly, quantification of Alizarin Red S that represents calcium deposition in cells and serves as a marker of osteogenic differentiation has demonstrated that the amount of mineralized matrix in 1-month old rat cells after incubation in osteogenic medium was approximately 10-fold higher compared to cells of old rats ($P<0.01$, unpaired t-test) (Fig. 3b). In turn, CASIN treatment enhanced the osteogenic differentiation of ADMSCs from aged rats by more than twice ($P<0.05$, unpaired t-test), yet this was not up to the levels seen in ADMSCs obtained from young rats (Fig. 3b).

CASIN reduces ERK1/2 and JNK phosphorylation in ADMSCs from aged rats

There is evidence suggesting the involvement of MAP kinases in MSC senescence and inhibition of their differentiation capacities (Bost et al. 2005; Jaiswal et al. 2000; Jin et al. 2010; Wang et al. 2005). In turn, Cdc42 has been shown to regulate MAPK/ERK signaling pathways under conditions of stress (Cheng et al. 2004; Lv et al. 2017; Wang et al. 2005). Thus, we measured the activation of ERK1/2 and c-Jun N-terminal kinase (JNK) in ADMSCs, and tested the effects of the Cdc42 inhibitor CASIN. Results obtained using the Meso Scale Discovery immunoassay demonstrated significantly increased phosphorylation of ERK1/2 and JNK in ADMSCs isolated from 24-month-old rats in comparison with cells isolated from 1 month old rats (Figs. 3c, 3d). As the activation of these kinases is via phosphorylation, this implies an increase in their activity. Treatment with CASIN significantly decreased the phosphorylation of ERK1/2 (63%) and JNK (65%) in ADMSCs from 24-month-old rats to levels similar to that seen in ADMSCs from young rats, implying reduced kinase activity (Figs. 3c, 3d).

Inhibition of Cdc42 in ADMSCs isolated from 24-month old rats by three different compounds

To confirm that all above mentioned effects of CASIN resulted directly from Cdc42 inhibition, and not due to inhibitor off-target effects, we applied two additional inhibitors of Cdc42 (ZCL278 and ML-141) and assessed their effects on proliferation capability and expression of SA-β-Gal in ADMSs isolated from 24 months old rats. Assessment of the Cdc42-GTP level by Western blot has confirmed inhibition of Cdc42 activity in aged ADMSCs by all three compounds (Fig. 4a). These inhibitors also resulted in a significant decrease in the percentage of SA-β-Gal-positive cells compared to untreated control ($P \leq 0.05$; unpaired t-test), with the most prominent effects seen with CASIN and ZCL278 (Fig. 4b and Supplementary Fig. 6). Using

CCK-8 analysis to assess ADMSC growth kinetics showed that CASIN, ML141 and ZCL278 improved the impaired proliferative activity of ADMSCs from aged rats (Fig. 4c).

Discussion

Cdc42, an abundant small Rho GTPase, is up-regulated in some age-related chronic diseases, tumors, and aging-associated cellular signaling pathways (Hooff et al. 2010; Ito et al. 2014; Kerber et al. 2009; Lee et al. 2014; Loirand et al. 2013; Raut et al. 2015; Stengel and Zheng 2011; Wang et al. 2007). There is data indicating that Cdc42 is involved in differentiation and proliferation of MSC (Gao et al. 2011; Jirong Wang 2014; Raggi and Berardi 2012; Shin et al. 2014). In the present study, we have investigated aging-associated Cdc42 activity in adipose-derived MSCs isolated from male rats of different ages and tested the effects of pharmacological inhibition of Cdc42 in MSCs isolated from aged animals. We focused on males in order to exclude gender effects since there is accumulating evidence that age-related alterations of mesenchymal stem cells can be modulated by sex hormones and estrogen decreases Cdc42 activity (Azios et al. 2007; Breu et al. 2011; Fossett et al. 2012; Kawagishi-Hotta et al. 2017). However, an important question remains whether the activity of Cdc42 plays similar role in aging processes of ADMSCs from female animals yet further research is needed to clarify this issue.

Results from this study show that the capability of adipose-derived MSCs (ADMSCs) from rats to proliferate decreases in proportion to the age of the animal. This reduced proliferative ability is associated with increased levels of activated Cdc42 and an increased proportion of SA-β-Gal stained cells, suggestive of cellular senescence. In addition, the multipotent differentiation ability of ADSMSCs reduces with increased animal age for the osteogenic, chrondrogenic and adipogenic cell lineages. These data suggest that an increasing proportion of MSCs show signs of cellular senescence with increasing rat age.

When ADMSCs isolated from rats at 24 months of age are cultured in the presence of three different inhibitors of Cdc42 activity they show a much improved proliferation capability and a significantly reduced staining for SA-β-Gal. These effects are associated with a reduction in the levels of activated Cdc42. The most effective inhibitor, CASIN, reduces SA-β-Gal staining to levels similar to that seen in ADMSCs from 6-month old rats. As these inhibitors are all chemically distinct and have distinct modes of action, with CASIN and ZCL278 competing with guanine nucleotide exchange factors and ML-141 non-competitively preventing GTP binding to Cdc42 (Lin and Zheng 2015), these data strongly suggest the improved proliferation and reduced SA-β-Gal staining result from Cdc42 inhibition, and are not due to inhibitor off-target effects. In

addition to elevated Cdc42-GTP levels, ADMSCs from 24-month old rats have elevated levels of the cyclin-dependent kinase inhibitor $p16^{INK4a}$, and elevated formation of F-actin stress fibres, both features of senescent cells (Guay et al. 1997; Liu et al. 2009). CASIN treatment reduced $p16^{INK4a}$ levels to that seen in ADMSCs from young rats, and increased the adipogenic and osteogenic differentiation ability of ADMSCs from aged rats and reduced actin polymerization in these cells, although this was not increased to the capability seen in ADMSCs from 1-month old animals.

Thus, it appears that ADMSCs isolated from 24-month old rats show several signs of increased cellular senescence and a reduction of differentiation potential compared to ADMSCs from younger animals that is due, at least in part, to elevated Cdc42, and that these effects increase with animal age. In addition, small molecule inhibition of Cdc42 activity can result in partial rejuvenation of ADMSCs from aged rats. These results concur with data from mouse that show increased active Cdc42 with age in various tissues (Xing et al. 2006), and that constitutively increased Cdc42 activity results in aging-like phenotypes in mouse hematopoietic stem cells (HSCs) (Florian et al. 2012). In the latter example, pharmacological reduction of Cdc42 activity using CASIN results in partial rejuvenation in the HSCs. In conclusion, the data demonstrate the involvement of Cdc42 activity in stem cell aging and suggest a common mechanism of aging is seen in different stem cell lineages.

So how does increased Cdc42 activity have these effects? One possibility is via the MAP kinase ERK1/2 and JNK signaling pathways that are involved in cellular senescence processes and whose activity increases during aging (Jones and Lancaster 2015; King et al. 2007; Mylabathula et al. 2006; Shin et al. 2005). The Cdc42 GTPases are involved in the regulation of ERK1/2 and JNK (Coso et al. 1995; Frost et al. 1997), suggesting that up-regulation of Cdc42-GTP activity may lead to increased cellular senescence via activation of these pathways. The ERK and JNK pathways are also implicated in differentiation of MSCs. For example, activation of ERK1/2 inhibits adipogenic differentiation in mouse cells whereas siRNA depletion of ERK1/2 increases this (Kim et al. 2007), and total and phosphorylated ERK1/2 levels are reduced at early stages of human MSC adipogenic differentiation (Donzelli et al. 2011). Moreover, there is data demonstrating that erythropoietin inhibits adipogenic differentiation of bone marrow derived mouse MSCs via activation of ERK (Liu et al. 2015). Finally, an inhibitory role has been demonstrated for JNK in both adipogenesis and osteogenesis in human MSCs (Gu et al. 2015; Tominaga et al. 2005). Thus, the increased aging and reduced differentiation capacity seen in ADMSCs from aged rats may be due to increased Cdc42 activity affecting the ERK1/2 and JNK signaling pathways. This idea is supported by the observation that phosphorylation of both ERK1/2 and JNK is increased in ADMSCs with animal age, and CASIN inhibition of

Cdc42 results in reduced cellular senescence and increased adipogenic and osteogenic differentiation potential associated with reduced activation of these kinases.

Studies have suggested that oxidative stress is a major factor accelerating cell senescence (Brandl et al. 2011; Davalli et al. 2016), and there is evidence for a critical role of NADPH oxidases-mediated ROS signaling pathways in aging process (Sahoo et al. 2016). In addition, suppression of NADPH oxidase by apocynin partially reversed the aging process and enhanced osteogenic potential of MSCs (Sun et al. 2015). Our results demonstrated that ROS production increased in ADMSCs from aged rats and that this was attenuated by CASIN. These data, together with the observation that Cdc42 regulates NADPH oxidase activation (Ascer et al. 2015; Qian et al. 2005; Wang et al. 2012b) suggests the possibility that inhibition of Cdc42 leads to an improvement of ADMSC proliferation and differentiation via suppression of NADPH oxidase activity.

Finally, it has been demonstrated that exposure of MSCs isolated from younger rats to serum from older animals inhibited cell proliferation and survival by activation of excessive Wnt/β-catenin cell signaling pathway (Zhang et al. 2011). In turn, activation of Wnt/β-catenin signaling induced a DNA damage response (Xu et al. 2008) leading to up-regulation of $p16^{INK4a}$, resulting in an induction of cellular aging (Kosar et al. 2011). As activation of $p16^{INK4a}$ can result from Cdc42 GTPase activation (Chen et al. 2013), and, according to our finding, inhibition of Cdc42 activity by CASIN decreases the expression of $P16^{INK4a}$, it is possible that the increased senescence seen in ADMSCs from aged rats results from up-regulated Wnt/β-catenin signaling, albeit this is speculation. However, possible support for this comes from data showing that non-canonical Wnt5a signaling can induce aging-associated phenotypes in HSCs from young mice via activation of Cdc42 (Florian et al. 2013).

In conclusion, our data demonstrate the involvement of Cdc42 in male rat mesenchymal stem cell aging and differentiation potential, although the precise mechanisms of Cdc42 action are not clearly understood and require further investigations. Understanding the basic molecular mechanisms underlying stem cell aging should provide new insights into the development of new strategies for rejuvenation treatment, regenerative medicine and stem cell therapy.

Acknowledgements

This work was supported by Grant No. 0114PK00489 from Ministry of Education and Science of the Republic of Kazakhstan and Grant No. 129-2017/022-2017 from Nazarbayev University. The funders played no role in the design or execution of this work, nor in the writing of this paper.

Conflict of interest statement

The authors declare no conflicts of interest

References

Arana M, Mazo M, Aranda P, Pelacho B, Prosper F (2013) Adipose tissue-derived mesenchymal stem cells: isolation, expansion, and characterization Methods Mol Biol 1036:47-61 doi:10.1007/978-1-62703-511-8_4

Ascer LG, Magalhaes YT, Espinha G, Osaki JH, Souza RC, Forti FL (2015) CDC42 Gtpase Activation Affects Hela Cell DNA Repair and Proliferation Following UV Radiation-Induced Genotoxic Stress J Cell Biochem 116:2086-2097 doi:10.1002/jcb.25166

Azios NG, Krishnamoorthy L, Harris M, Cubano LA, Cammer M, Dharmawardhane SF (2007) Estrogen and Resveratrol Regulate Rac and Cdc42 Signaling to the Actin Cytoskeleton of Metastatic Breast Cancer Cells Neoplasia (New York, NY) 9:147-158

Bony C, Cren M, Domergue S, Toupet K, Jorgensen C, Noel D (2015) Adipose Mesenchymal Stem Cells Isolated after Manual or Water-jet-Assisted Liposuction Display Similar Properties Front Immunol 6:655 doi:10.3389/fimmu.2015.00655

Bost F, Aouadi M, Caron L, Binetruy B (2005) The role of MAPKs in adipocyte differentiation and obesity Biochimie 87:51-56 doi:10.1016/j.biochi.2004.10.018

Brandl A, Meyer M, Bechmann V, Nerlich M, Angele P (2011) Oxidative stress induces senescence in human mesenchymal stem cells Exp Cell Res 317:1541-1547 doi:10.1016/j.yexcr.2011.02.015

Breu A et al. (2011) Estrogen reduces cellular aging in human mesenchymal stem cells and chondrocytes J Orthop Res 29:1563-1571 doi:10.1002/jor.21424

Chandrasekaran A, Idelchik M, Melendez JA (2017) Redox control of senescence and age-related disease Redox Biol 11:91-102 doi:10.1016/j.redox.2016.11.005

Chen HH, Decot V, Ouyang JP, Stoltz JF, Bensoussan D, de Isla NG (2009) In vitro initial expansion of mesenchymal stem cells is influenced by the culture parameters used in the isolation process Bio-medical materials and engineering 19:301-309 doi:10.3233/bme-2009-0595

Chen YW, Chu HC, Ze-Shiang L, Shiah WJ, Chou CP, Klimstra DS, Lewis BC (2013) p16 Stimulates CDC42-dependent migration of hepatocellular carcinoma cells PLoS One 8:e69389 doi:10.1371/journal.pone.0069389

Cheng M, Chen Y, Xiao W, Sun R, Tian Z (2013) NK cell-based immunotherapy for malignant diseases Cell Mol Immunol 10:230-252 doi:10.1038/cmi.2013.10

Cheng T-L, Symons M, Jou T-S (2004) Regulation of anoikis by Cdc42 and Rac1 Experimental Cell Research 295:497-511 doi:http://dx.doi.org/10.1016/j.yexcr.2004.02.002

Chretien A et al. (2008) Role of TGF-beta1-independent changes in protein neosynthesis, p38alphaMAPK, and cdc42 in hydrogen peroxide-induced senescence-like morphogenesis Free Radic Biol Med 44:1732-1751 doi:10.1016/j.freeradbiomed.2008.01.026

Colavitti R, Finkel T (2005) Reactive oxygen species as mediators of cellular senescence IUBMB life 57:277-281 doi:10.1080/15216540500091890

Coso OA et al. (1995) The small GTP-binding proteins Rac1 and Cdc42 regulate the activity of the JNK/SAPK signaling pathway Cell 81:1137-1146

Dai LJ, Li HY, Guan LX, Ritchie G, Zhou JX (2009) The therapeutic potential of bone marrow-derived mesenchymal stem cells on hepatic cirrhosis Stem Cell Res 2:16-25 doi:10.1016/j.scr.2008.07.005

Davalli P, Mitic T, Caporali A, Lauriola A, D'Arca D (2016) ROS, Cell Senescence, and Novel Molecular Mechanisms in Aging and Age-Related Diseases Oxid Med Cell Longev 2016:3565127 doi:10.1155/2016/3565127

Donzelli E, Lucchini C, Ballarini E, Scuteri A, Carini F, Tredici G, Miloso M (2011) ERK1 and ERK2 are involved in recruitment and maturation of human mesenchymal stem cells induced to adipogenic differentiation J Mol Cell Biol 3:123-131 doi:10.1093/jmcb/mjq050

Fernandez Vallone VB, Romaniuk MA, Choi H, Labovsky V, Otaegui J, Chasseing NA (2013) Mesenchymal stem cells and their use in therapy: what has been achieved? Differentiation 85:1-10 doi:10.1016/j.diff.2012.08.004

Florian MC et al. (2012) Cdc42 activity regulates hematopoietic stem cell aging and rejuvenation Cell Stem Cell 10:520-530 doi:10.1016/j.stem.2012.04.007

Florian MC et al. (2013) A canonical to non-canonical Wnt signalling switch in haematopoietic stem-cell ageing Nature 503:392-396 doi:10.1038/nature12631

Fossett E, Khan WS, Longo UG, Smitham PJ (2012) Effect of age and gender on cell proliferation and cell surface characterization of synovial fat pad derived mesenchymal stem cells J Orthop Res 30:1013-1018 doi:10.1002/jor.22057

Frost JA, Steen H, Shapiro P, Lewis T, Ahn N, Shaw PE, Cobb MH (1997) Cross-cascade activation of ERKs and ternary complex factors by Rho family proteins EMBO J 16:6426-6438 doi:10.1093/emboj/16.21.6426

Gao L, Gorski JL, Chen CS (2011) The Cdc42 guanine nucleotide exchange factor FGD1 regulates osteogenesis in human mesenchymal stem cells Am J Pathol 178:969-974 doi:10.1016/j.ajpath.2010.11.051

Gu H et al. (2015) Role of c-Jun N-terminal kinase in the osteogenic and adipogenic differentiation of human adipose-derived mesenchymal stem cells Exp Cell Res 339:112-121 doi:10.1016/j.yexcr.2015.08.005

Guay J, Lambert H, Gingras-Breton G, Lavoie JN, Huot J, Landry J (1997) Regulation of actin filament dynamics by p38 map kinase-mediated phosphorylation of heat shock protein 27 J Cell Sci 110 (Pt 3):357-368

Hooff GP, Wood WG, Muller WE, Eckert GP (2010) Isoprenoids, small GTPases and Alzheimer's disease Biochim Biophys Acta 1801:896-905 doi:10.1016/j.bbalip.2010.03.014

Ito TK et al. (2014) A crucial role for CDC42 in senescence-associated inflammation and atherosclerosis PLoS One 9:e102186 doi:10.1371/journal.pone.0102186

Jaiswal RK, Jaiswal N, Bruder SP, Mbalaviele G, Marshak DR, Pittenger MF (2000) Adult human mesenchymal stem cell differentiation to the osteogenic or adipogenic lineage is regulated by mitogen-activated protein kinase J Biol Chem 275:9645-9652

Jin Y et al. (2010) Mesenchymal stem cells cultured under hypoxia escape from senescence via down-regulation of p16 and extracellular signal regulated kinase Biochemical and Biophysical Research Communications 391:1471-1476 doi:http://dx.doi.org/10.1016/j.bbrc.2009.12.096

Jirong Wang YGCX (2014) The roles of CDC42 in bone development. Paper presented at the the European Calcified Tissue Society Conference ECTS 2014 Prague,Czech Republic,

Jones SA, Lancaster MK (2015) Progressive age-associated activation of JNK associates with conduction disruption in the aged atrium Mech Ageing Dev 146-148:72-80 doi:10.1016/j.mad.2015.05.001

Kasper G et al. (2009) Insights into mesenchymal stem cell aging: involvement of antioxidant defense and actin cytoskeleton Stem Cells 27:1288-1297 doi:10.1002/stem.49

Kawagishi-Hotta M et al. (2017) Enhancement of individual differences in proliferation and differentiation potentials of aged human adipose-derived stem cells Regenerative Therapy 6:29-40 doi:https://doi.org/10.1016/j.reth.2016.12.004

Kerber RA, O'Brien E, Cawthon RM (2009) Gene expression profiles associated with aging and mortality in humans Aging Cell 8:239-250 doi:10.1111/j.1474-9726.2009.00467.x

Kim KA, Kim JH, Wang Y, Sul HS (2007) Pref-1 (preadipocyte factor 1) activates the MEK/extracellular signal-regulated kinase pathway to inhibit adipocyte differentiation Mol Cell Biol 27:2294-2308 doi:10.1128/MCB.02207-06

King AM, Van der Put E, Blomberg BB, Riley RL (2007) Accelerated Notch-dependent degradation of E47 proteins in aged B cell precursors is associated with increased ERK MAPK activation J Immunol 178:3521-3529

Kosar M, Bartkova J, Hubackova S, Hodny Z, Lukas J, Bartek J (2011) Senescence-associated heterochromatin foci are dispensable for cellular senescence, occur in a cell type- and insult-

dependent manner and follow expression of p16(ink4a) Cell Cycle 10:457-468 doi:10.4161/cc.10.3.14707
Kramer J, Dazzi F, Dominici M, Schlenke P, Wagner W (2012) Clinical perspectives of mesenchymal stem cells Stem Cells Int 2012:684827 doi:10.1155/2012/684827
Lee CC, Ye F, Tarantal AF (2006) Comparison of growth and differentiation of fetal and adult rhesus monkey mesenchymal stem cells Stem Cells Dev 15:209-220 doi:10.1089/scd.2006.15.209
Lee S, Craig BT, Romain CV, Qiao J, Chung DH (2014) Silencing of CDC42 inhibits neuroblastoma cell proliferation and transformation Cancer Lett 355:210-216 doi:10.1016/j.canlet.2014.08.033
Li Z et al. (2017) Aging-Impaired Filamentous Actin Polymerization Signaling Reduces Alveolar Macrophage Phagocytosis of Bacteria Journal of immunology (Baltimore, Md : 1950) 199:3176-3186 doi:10.4049/jimmunol.1700140
Lin Y, Zheng Y (2015) Approaches of targeting Rho GTPases in cancer drug discovery Expert Opin Drug Discov 10:991-1010 doi:10.1517/17460441.2015.1058775
Liu GX, Zhu JC, Chen XY, Zhu AZ, Liu CC, Lai Q, Chen ST (2015) Inhibition of adipogenic differentiation of bone marrow mesenchymal stem cells by erythropoietin via activating ERK and P38 MAPK Genet Mol Res 14:6968-6977 doi:10.4238/2015.June.26.5
Liu Y et al. (2009) Expression of p16(INK4a) in peripheral blood T-cells is a biomarker of human aging Aging Cell 8:439-448 doi:10.1111/j.1474-9726.2009.00489.x
Loirand G, Sauzeau V, Pacaud P (2013) Small G proteins in the cardiovascular system: physiological and pathological aspects Physiol Rev 93:1659-1720 doi:10.1152/physrev.00021.2012
Lotfy A, Salama M, Zahran F, Jones E, Badawy A, Sobh M (2014) Characterization of mesenchymal stem cells derived from rat bone marrow and adipose tissue: a comparative study Int J Stem Cells 7:135-142 doi:10.15283/ijsc.2014.7.2.135
Lv J et al. (2017) Cdc42 regulates LPS-induced proliferation of primary pulmonary microvascular endothelial cells via ERK pathway Microvascular Research 109:45-53 doi:http://dx.doi.org/10.1016/j.mvr.2016.10.001
Maredziak M, Marycz K, Tomaszewski KA, Kornicka K, Henry BM (2016) The Influence of Aging on the Regenerative Potential of Human Adipose Derived Mesenchymal Stem Cells Stem Cells Int 2016:2152435 doi:10.1155/2016/2152435
Mareschi K et al. (2006) Expansion of mesenchymal stem cells isolated from pediatric and adult donor bone marrow J Cell Biochem 97:744-754 doi:10.1002/jcb.20681
McGrail DJ, Ghosh D, Quach ND, Dawson MR (2012) Differential mechanical response of mesenchymal stem cells and fibroblasts to tumor-secreted soluble factors PLoS One 7:e33248 doi:10.1371/journal.pone.0033248
Mylabathula DB, Rice KM, Wang Z, Uddemarri S, Kinnard RS, Blough ER (2006) Age-associated changes in MAPK activation in fast- and slow-twitch skeletal muscle of the F344/NNiaHSD X Brown Norway/BiNia rat model Exp Gerontol 41:205-214 doi:10.1016/j.exger.2005.11.001
Qian Y, Liu KJ, Chen Y, Flynn DC, Castranova V, Shi X (2005) Cdc42 regulates arsenic-induced NADPH oxidase activation and cell migration through actin filament reorganization J Biol Chem 280:3875-3884 doi:10.1074/jbc.M403788200
Raggi C, Berardi AC (2012) Mesenchymal stem cells, aging and regenerative medicine Muscles, Ligaments and Tendons Journal 2:239-242
Raut SK et al. (2015) miR-30c Mediates Upregulation of Cdc42 and Pak1 in Diabetic Cardiomyopathy Cardiovasc Ther 33:89-97 doi:10.1111/1755-5922.12113
Sahoo S, Meijles DN, Pagano PJ (2016) NADPH oxidases: key modulators in aging and age-related cardiovascular diseases? Clin Sci (Lond) 130:317-335 doi:10.1042/CS20150087
Sethe S, Scutt A, Stolzing A (2006) Aging of mesenchymal stem cells Ageing Res Rev 5:91-116 doi:10.1016/j.arr.2005.10.001
Shin KK, Kim YS, Kim JY, Bae YC, Jung JS (2014) miR-137 controls proliferation and differentiation of human adipose tissue stromal cells Cell Physiol Biochem 33:758-768 doi:10.1159/000358650
Shin MH et al. (2005) H2O2 accumulation by catalase reduction changes MAP kinase signaling in aged human skin in vivo J Invest Dermatol 125:221-229

Sotiropoulou PA, Perez SA, Salagianni M, Baxevanis CN, Papamichail M (2006) Characterization of the optimal culture conditions for clinical scale production of human mesenchymal stem cells Stem Cells 24:462-471 doi:10.1634/stemcells.2004-0331

Stengel K, Zheng Y (2011) Cdc42 in oncogenic transformation, invasion, and tumorigenesis Cell Signal 23:1415-1423 doi:10.1016/j.cellsig.2011.04.001

Sun J, Ming L, Shang F, Shen L, Chen J, Jin Y (2015) Apocynin suppression of NADPH oxidase reverses the aging process in mesenchymal stem cells to promote osteogenesis and increase bone mass Sci Rep 5:18572 doi:10.1038/srep18572

Tang DD, Gunst SJ (2004) The small GTPase Cdc42 regulates actin polymerization and tension development during contractile stimulation of smooth muscle The Journal of biological chemistry 279:51722-51728 doi:10.1074/jbc.M408351200

Tominaga S, Yamaguchi T, Takahashi S, Hirose F, Osumi T (2005) Negative regulation of adipogenesis from human mesenchymal stem cells by Jun N-terminal kinase Biochem Biophys Res Commun 326:499-504 doi:10.1016/j.bbrc.2004.11.056

Wang L, Yang L, Burns K, Kuan CY, Zheng Y (2005) Cdc42GAP regulates c-Jun N-terminal kinase (JNK)-mediated apoptosis and cell number during mammalian perinatal growth Proc Natl Acad Sci U S A 102:13484-13489 doi:10.1073/pnas.0504420102

Wang L, Yang L, Debidda M, Witte D, Zheng Y (2007) Cdc42 GTPase-activating protein deficiency promotes genomic instability and premature aging-like phenotypes Proc Natl Acad Sci U S A 104:1248-1253 doi:10.1073/pnas.0609149104

Wang S, Qu X, Zhao RC (2012a) Clinical applications of mesenchymal stem cells J Hematol Oncol 5:19 doi:10.1186/1756-8722-5-19

Wang X et al. (2012b) Cdc42-dependent activation of NADPH oxidase is involved in ethanol-induced neuronal oxidative stress PLoS One 7:e38075 doi:10.1371/journal.pone.0038075

Xing Z et al. (2006) Increased hematopoietic stem cell mobilization in aged mice Blood 108:2190-2197 doi:10.1182/blood-2005-12-010272

Xu M, Yu Q, Subrahmanyam R, Difilippantonio MJ, Ried T, Sen JM (2008) Beta-catenin expression results in p53-independent DNA damage and oncogene-induced senescence in prelymphomagenic thymocytes in vivo Mol Cell Biol 28:1713-1723 doi:10.1128/MCB.01360-07

Xu XP et al. (2017) Ang II-AT2R increases mesenchymal stem cell migration by signaling through the FAK and RhoA/Cdc42 pathways in vitro Stem Cell Res Ther 8:164 doi:10.1186/s13287-017-0617-z

Yue B, Lu B, Dai KR, Zhang XL, Yu CF, Lou JR, Tang TT (2005) BMP2 gene therapy on the repair of bone defects of aged rats Calcif Tissue Int 77:395-403 doi:10.1007/s00223-005-0180-y

Zhang DY, Wang HJ, Tan YZ (2011) Wnt/beta-catenin signaling induces the aging of mesenchymal stem cells through the DNA damage response and the p53/p21 pathway PLoS One 6:e21397 doi:10.1371/journal.pone.0021397

Zlotorynski E (2015) Communicating with senescence Nat Rev Mol Cell Biol 16:267

Figure Legends

Fig. 1 Properties of ADMSCs isolated from rats of different ages (n=25, 5 rats per group). **a** Quantitative analysis of Oil red O stained ADMSCs; data shown as Mean ± SD, *P<0.05 (unpaired t-test). **b** Proliferative activity as assessed by CCK-8 assay plotted as optical density versus days. CCK-8 assay: two-way ANOVA with post hoc analysis (F=53.24, df=4); **** p<0.0001 (1 month vs 3, 6, 12, >24 month; 3 month vs >24 month); *** p<0.0003 (6 month vs 3

month); ns – not significant (>24 month vs 6, 12 month). **c** Bar chart showing percenatge of ADMSCs staining for SA-β-Galactosidase activity; $P \leq 0.001$ (one way ANOVA and regression analysis). **d** Western blot depicting levels of active and total Cdc42. **e** Quantification analysis of Cdc42-GTP/tottal Cdc42; $*P \leq 0.05$ (unpaired t-test).

Fig. 2 Properties of CASIN treated ADMSCs from 1 months old (YOUNG) and 24 month old (OLD) rats (n=20, 5 rats per group). **a** Western blot depicting levels of active and total Cdc42 and total P16INK4a in Cdc42 inhibitor treated ADMSCs compared to the untreated controls. **b** Quantification ratio of the Cdc42-GTP/total Cdc42; $*p \leq 0.05$ (unpaired t-test). **c** Quantitative analysis of the total P16INK4a; $*p \leq 0.05$ (unpaired t-test). **d** Percentage of SA-β-Gal-positive ADMSCs in the experimental and control (untreated) groups; $*p \leq 0.05$, $***p \leq 0.001$(unpaired t-test). **e,f** Proliferative activity of Cdc42 inhibitor treated ADMSCs compared to untreated controls as assessed by CCK-8 assay. **g** ROS levels in ADMSCs isolated from 1 month old and 24 months old rats; $*p \leq 0.05$, $***p \leq 0.001$ (unpaired t-test). **h** Actin polymerization in ADMSCs isolated from 1 month old and 24 months old rats; $*p \leq 0.05$, $***p \leq 0.001$ (unpaired t-test).

Fig. 3 Properties of CASIN treated ADMSCs from aged rats (n=15, 5 rats per group). **a** Adipogenic differentiation of CASIN treated ADMSCs from aged rats (CASIN) compared to untreated ADMSCs from aged (OLD) and 1 month old (YOUNG) rats. Quantitative analysis of Oil red O stained cells; data shown as Mean ± SD, $*P<0.05$ (unpaired t-test).**b** Quantitative colorimetric results of Alizarin Red S staining for osteogenic differentiation; data shown as Mean ± SD, $**P<0.01$, $*P<0.05$ (unpaired t-test). **c**, **d** Ratio of pERK1/2:ERK1/2 levels (**c**) and pJNK:JNK levels (**d**) in CASIN treated ADMSCs from aged rats (CASIN) compared to untreated ADMSCs from aged (OLD) and 1 month old (YOUNG) rats. Data shown as Mean ± SD, $*P<0.05$ (unpaired t-test).

Fig.4 Inhibition of Cdc42 by different compounds in ADMSCs isolated from 24 months old rats (n=20, 5 rats per group). **a** Western blot depicting levels of active and total Cdc42 in aged MSCS after treatment with three different Cdc42 inhibitors. **b** percentage of SA-β-Gal-positive ADMSCs in the experimental and control (untreated) groups; *$p \leq 0.05$ (unpaired t-test). **c** CCK-8 assay: two-way ANOVA with post-hoc analysis (: $F=50.79$, $df=3$), ****$P < 0.0001$ vs control.

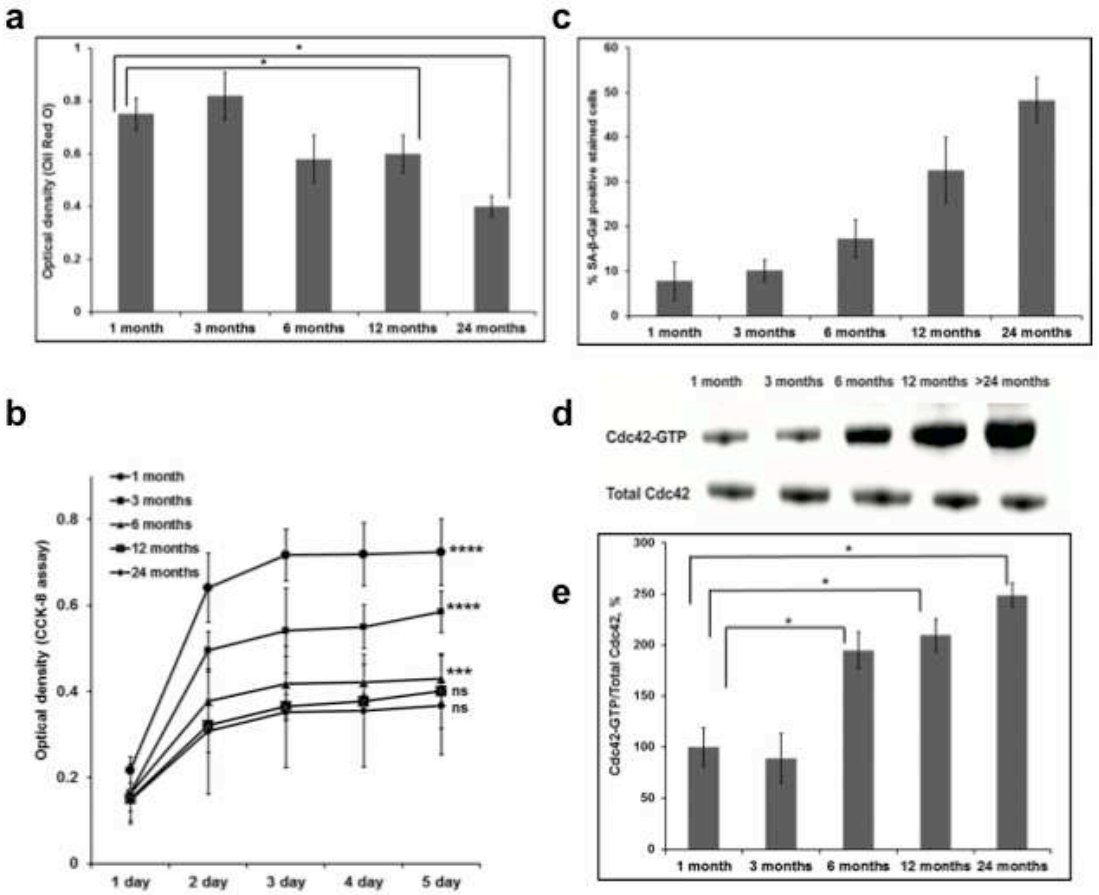
a
Optical density (Oil Red O)
1 month
3 months
6 months
12 months
24 months
c
% SA-β-Gal positive stained cells
1 month
3 months
6 months
12 months
24 months
b
Optical density (CCK-8 assay)
1 month
3 months
6 months
12 months
24 months
1 day
2 day
3 day
4 day
5 day
****
****
***
ns
ns
d
1 month
3 months
6 months
12 months
>24 months
Cdc42-GTP
Total Cdc42
e
Cdc42-GTP/Total Cdc42, %
1 month
3 months
6 months
12 months
24 months

Fig.1

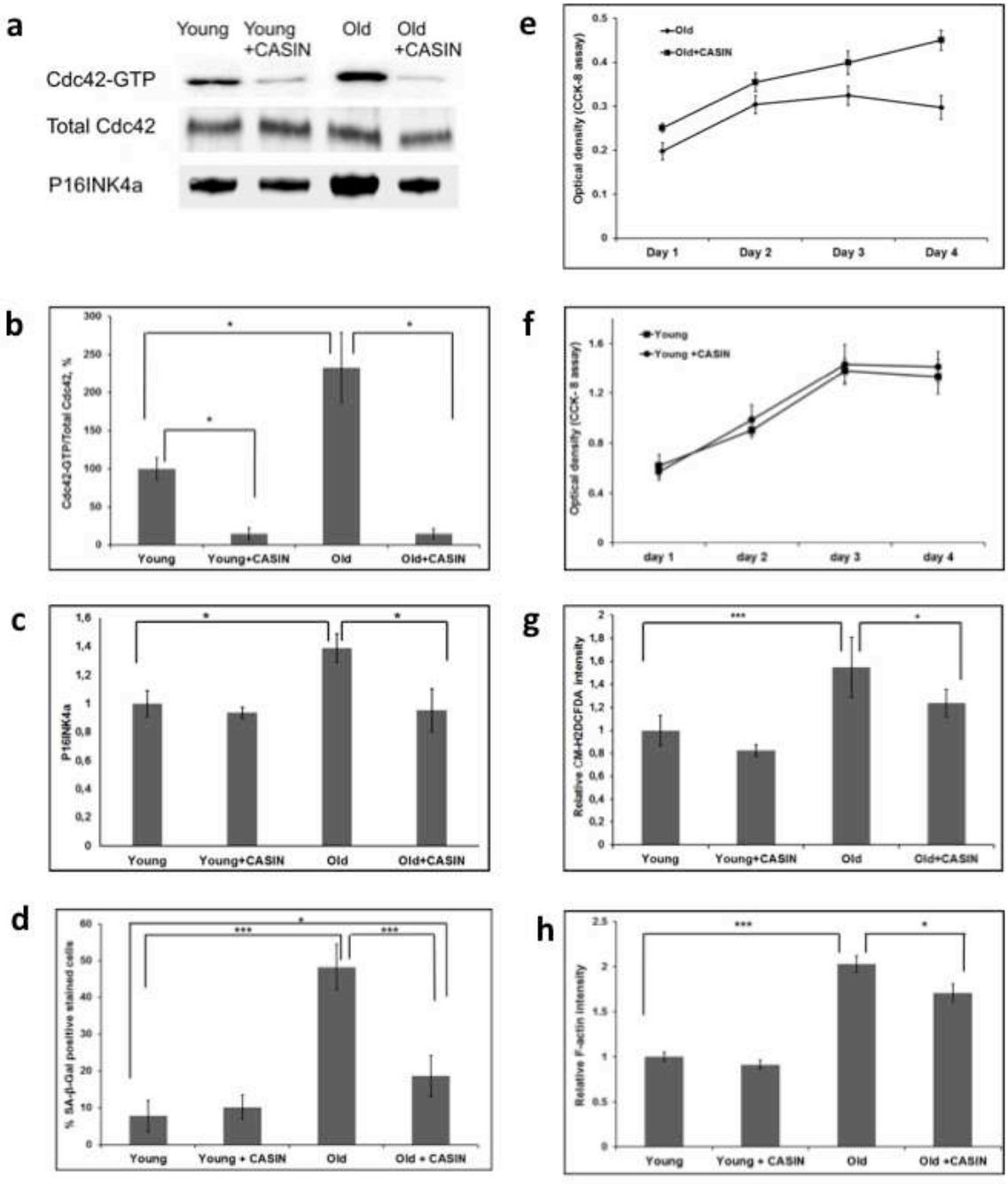
a
Young
Young +CASIN
Old
Old +CASIN
Cdc42-GTP
Total Cdc42
P16INK4a
b
Cdc42-GTP/Total Cdc42, %
Young
Young+CASIN
Old
Old+CASIN
c
P16INK4a
d
% SA-β-Gal positive stained cells
Young + CASIN
e
Optical density (CCK-8 assay)
Old
Old+CASIN
Day 1
Day 2
Day 3
Day 4
f
Young
Young +CASIN
day 1
day 2
day 3
day 4
g
Relative CM-H2DCFDA intensity
h
Relative F-actin intensity

Fig.2

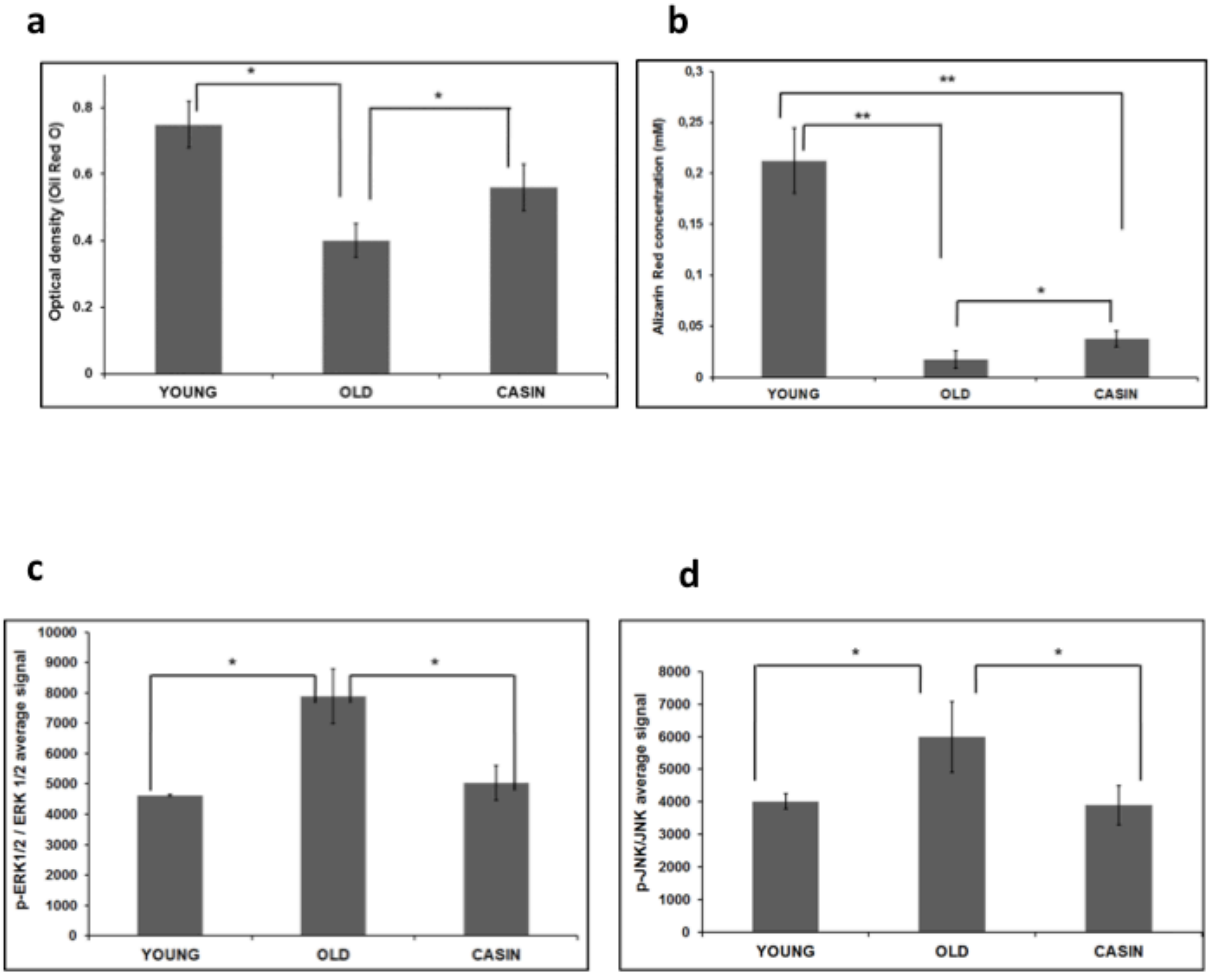
a
b
Optical density (Oil Red O)
0
0.2
0.4
0.6
0.8
*
*
YOUNG
OLD
CASIN
Alizarin Red concentration (mM)
0
0,05
0,1
0,15
0,2
0,25
0,3
**
**
*
YOUNG
OLD
CASIN
c
d
p-ERK1/2 / ERK 1/2 average signal
0
1000
2000
3000
4000
5000
6000
7000
8000
9000
10000
*
*
YOUNG
OLD
CASIN
p-JNK/JNK average signal
0
1000
2000
3000
4000
5000
6000
7000
8000
*
*
YOUNG
OLD
CASIN

Fig.3

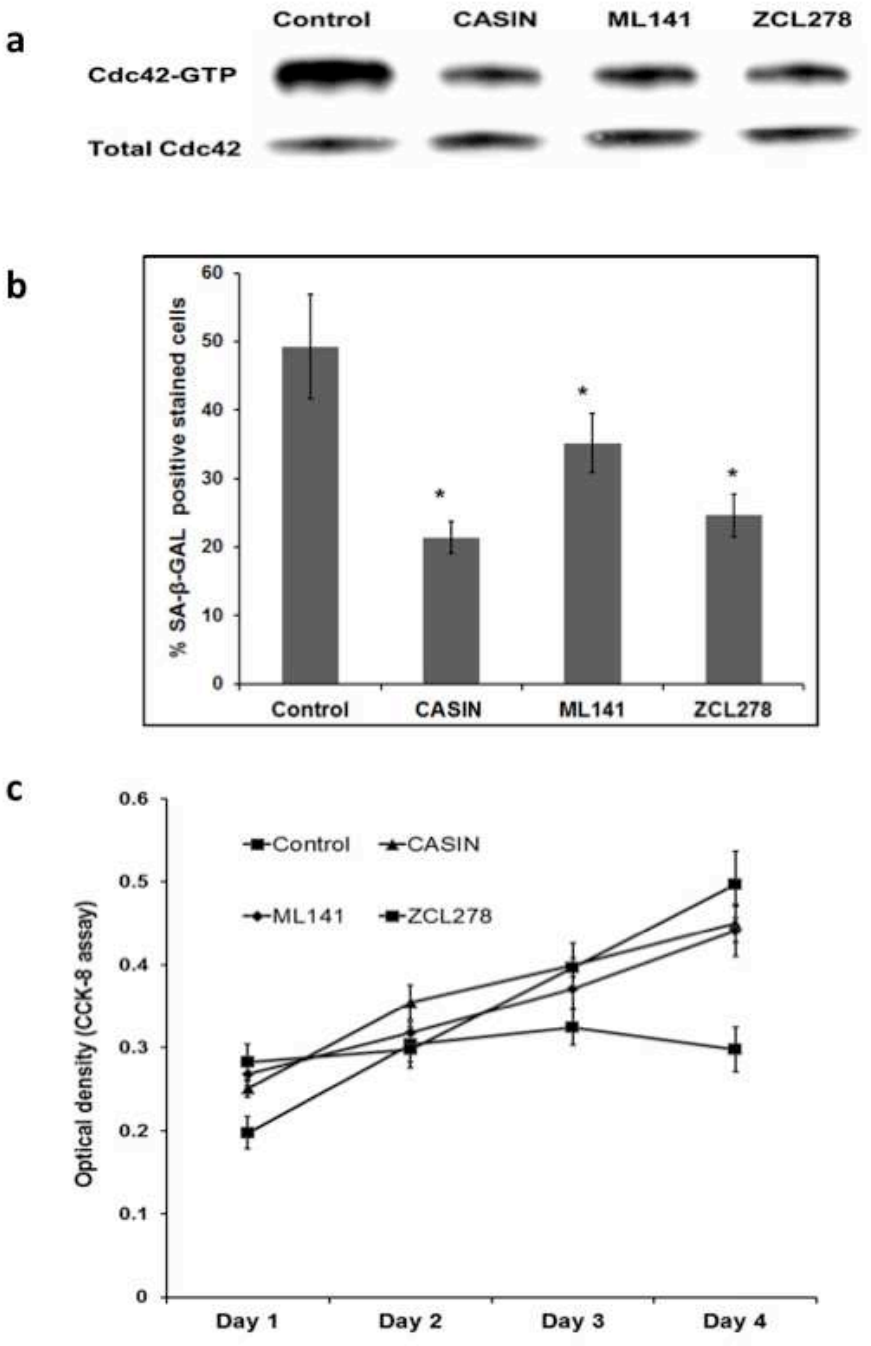
a
Control
CASIN
ML141
ZCL278
Cdc42-GTP
Total Cdc42
b
% SA-β-GAL positive stained cells
60
50
40
30
20
10
0
Control
CASIN
ML141
ZCL278
c
Optical density (CCK-8 assay)
0.6
0.5
0.4
0.3
0.2
0.1
0
Control
CASIN
ML141
ZCL278
Day 1
Day 2
Day 3
Day 4

Fig.4